Rate Constant for the Reaction of O with H$_2$ at High Temperature by Resonance Absorption Measurements of O Atoms

S. JAVOY, V. NAUDET, S. ABID, C. E. PAILLARD

Laboratoire de Combustion et Systèmes Réactifs, UPR n°421 CNRS 1C, Avenue de la Recherche Scientifique, 45071 Orléans Cedex 2, France

ABSTRACT: Resonance Absorption Spectroscopy (ARAS) has been used to measure O-atom concentration behind reflected shock waves in the temperature range 2690–3360 K at total pressures of about 250 kPa and using mixtures of N$_2$O and H$_2$ highly diluted in Ar. For the chosen experimental conditions, only a few elementary reactions exerted an appreciable influence on the O-atom profile so that the rate coefficient k_2 for the reaction O + H$_2$ → OH + H, directly responsible for the oxygen atom concentration decrease could be deduced by comparison between the experiment and computed simulation. In the actual temperature range we found: k_2(cm^3 mol^{-1} s^{-1}) = 9.25 × 10^{14} exp($-$9740/T(K)), with a percentage standard deviation of 8%. The influence of experimental uncertainties is discussed. This rate constant is compared with those reported previously in the literature. © 2000 John Wiley & Sons, Inc. Int J Chem Kinet 32: 686–695, 2000

INTRODUCTION

The optimization of thermal energy use and the limitation of pollutant impacts on the environment motivate research about chemical kinetic mechanisms in combustion. Rate coefficients for the elementary reactions must be determined precisely in order to simulate combustion processes. The slightly endothermic elementary reaction ($\Delta H^{\circ}_{298} = 8$ kJ mol^{-1}) of oxygen atom with the hydrogen molecule, O + H$_2$ → OH + H, plays a prominent role as part of the main chain-branching processes in the high-temperature combustion of hydrocarbons.

The rate constant for this reaction has been the subject of several experimental and theoretical studies over the last 40 years for various temperature ranges from 297 to 3532 K. The literature experimental results obtained at high temperature show a scattering of the rate-constant values, and we noted that only one investigation has been carried out at temperatures higher than 2700 K. In 1987 Natarajan and Roth [1] obtained by Resonance Absorption of O and H atoms over the temperature range 1713–3532 K the following three-parameter expression: k_2(cm^3 mol^{-1} s^{-1}) = 3.72 × 10^{6}T$^{2.17}$(K) exp($-$4080/T(K)), which agreed very well with results reported by other investigators at lower temperature ranges [2,3] and with the recommended expression of Baulch et al. [4]. Recently, Ryu et al. [5] confirmed the rate expressions proposed

earlier by Sutherland et al. [6] and Frank and Just [7]: k_2(cm^3 mol^{-1} s^{-1}) = 1.88×10^{14} exp($-6897/T$(K)), who found lower rate coefficients than authors previously quoted. This rate coefficient is in agreement with the theoretical calculations of Bowman et al. [8] and Garrett and Truhlar [9], realized at lower temperatures (250–2400 K). Yang et al. [10] proposed intermediate k_2 values between those of Natarajan and Roth [1] and Ryu et al. [5]: k_2(cm^3 mol^{-1} s^{-1}) = 3.7×10^{14} exp($-7818/T$(K)).

Because of the experimental results scattering in the literature and the lack of values at temperatures over 2700 K, it was important to reevaluate the rate constant of the O + H$_2 \rightarrow$ OH + H reaction at high temperature. The shock tube technique coupled with Atomic Resonance Absorption Spectroscopy has been used to measure O-atom concentration in the temperature range 2690–3360 K and at total pressures of about 250 kPa. The high sensitivity of the ARAS technique allows the use of very low initial reactant concentrations so that the temperature during the measuring time can be considered as constant and the secondary reaction importance can be assumed to be limited. The ARAS system used for this study was validated from a high-temperature chemical kinetic study of the O$_2$ dissociation and the O-atom recombination [11]. In the actual experimental conditions, the O atoms were generated by the fast thermal decomposition of N$_2$O, and the reaction with H$_2$ was directly responsible for the decrease in oxygen atom concentration. The rate constant for reaction (2) was deduced by comparison between experimental O-atom profiles and computed simulations.

The present result is compared to those from earlier experimental works and theoretical calculations.

EXPERIMENTAL

Details of the shock tube as well as the optical set-up have been described elsewhere [11] and only a short summary will be presented below.

The Shock Tube

All the N$_2$O/H$_2$/Ar experiments were obtained behind reflected shock waves in a 78-mm inner diameter stainless steel shock tube with a 0.9-m driver section and a 4-m long driven section. An oil diffusion pump with a water-cooled baffle evacuated the test section to less than 2×10^{-7} mbar and the typical leak-plus-outgassing rate was of the order of 8×10^{-7} mbar/min or less. A liquid nitrogen trap, smooth internal surface, and the ability to heat the shock tube up to 100°C approximated a high-purity shock tube. Helium was used as driver gas and the shock wave was initiated by the bursting of a double diaphragm. Temperature and pressure behind the reflected shock wave were computed from the incident shock speed, which was measured by four piezo-electric pressure gauges placed at known distances along the test section. We used one-dimension shock equations assuming complete vibrational equilibrium. Moreover, the exact compositions were used to compute shocked-gas properties from the measured shock velocity. The experimental observation duration was at least of 300 μs.

Gas Mixtures

Mixtures of N$_2$O and H$_2$ highly diluted in Ar were prepared by partial pressures and stored in a 10-l glass bulb. Because of the high sensitivity of the ARAS technique, all gases were of ultra-high purity: Ar > 99.9999%, H$_2$ > 99.9999%, and N$_2$O > 99.998%, and the glass preparation system was pumped down to 2×10^{-7} mbar by a turbomolecular pump.

Optical Arrangement

Atomic Resonance Absorption Spectroscopy was used to monitor O-atom profiles at the emission line of the O triplet at 130.5 nm. A microwave-excited discharge lamp that contained a flowing mixture of 1% O$_2$ in He maintained at a pressure of 3 Torr was used as light source for the absorption measurements. This lamp consisted of a 2.45 GHz microwave generator operating at 70 W power level. A vacuum UV monochromator was used to isolate the O-triplet wavelength, and a special blind photomultiplier was used to convert VUV photons. The operating conditions were chosen to minimize noise and reflected power without significant loss of signal strength. The absorption measurements were made behind a reflected shock front through two thin MgF$_2$ windows, close (10 mm) to the end of the driven section of the shock tube. MgF$_2$ material offers good transmission and is less sensitive to light-exposure effects. The spectral shape of the emitter line is not known in detail and is assumed to be mainly influenced by self-absorption or self-reversal. So calibration experiments were necessary to find a correlation between resonance absorption measurements and O-atom concentrations. The O-ARAS calibration depends on adjustable parameters such as lamp power, pressure in the lamp, and O$_2$/He mixture dilution. The shock tube and associated equipment are shown schematically in Figure 1.
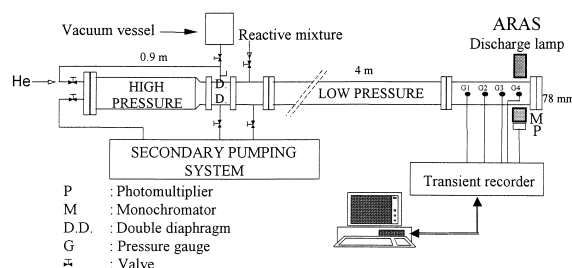
Figure 1   Experimental apparatus.

O-Atom Concentration Calibration

For O-atom calibration, the total thermal decomposition of N_2O behind reflected shock waves in N_2O/Ar mixtures was used. At temperatures above 2200 K, N_2O dissociation is very fast and recombination reactions as well as secondary reactions involving oxygen atoms that are known to be slow can be neglected. Thus, a steady-state concentration of O atoms is achieved within the observation time [12]. The atomic absorption cross section was determined experimentally with different gas mixtures containing 1.2–24.5 ppm of N_2O in Argon, shock heated in the temperature range 2540–3970 K and for pressure between 190 and 280 kPa. In our experimental conditions, we obtained the modified Lambert-Beer law:

$$A = 1 - \exp(-1.375 \times 10^{-10} \times \ell \times [O]^{0.66})$$

A is the absorption, ℓ the optical path in cm, and [O] the O-atom concentration in atoms cm^{-3}. The modified Lambert-Beer law ($[O]^n$, $n \neq 1$) was used to increase the concentration range. The calibration curve is illustrated in Figure 2. Our optical set-up allowed the measurement of O-atom absorption in the range of 20 to 85% and a corresponding O-atom concentration range of 4×10^{12} to 1.2×10^{14} atoms cm^{-3}.

RESULTS

The reaction between the oxygen atom and the hydrogen molecule, $O + H_2 \rightarrow OH + H$ (2) was studied behind reflected shock waves in a temperature range 2690–3360 K and at total pressures between 240 and 280 kPa. The different test gas mixtures of N_2O and H_2 highly diluted in Ar are given in Table I. Nearly 30 individual experiments were made and O-atom resonance absorption was recorded in each case. Then the O absorption record was translated into corresponding O-atom profiles with the modified Lambert-Beer law
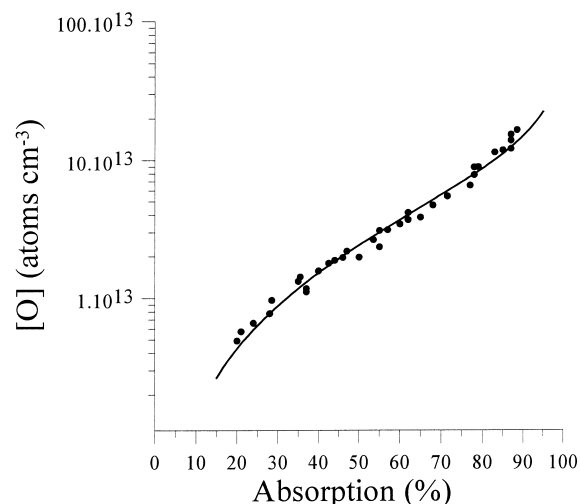

Figure 2   ARAS calibration curve for O atoms.

found previously. The rate-constant value for the studied reaction was determined from the best fit between computed and experimental concentration profiles.

Reaction Mechanism

The full reaction mechanism used for the computed simulations (SENKIN II [13]) is given in Table II. It was based on the detailed reaction mechanism implying the H, O, and Ar atoms used by Catoire et al. [14]. Some of the rate-coefficient expressions were taken from standard compilations [4,15–17]. $O_2 + Ar \rightarrow 2O + Ar$ (18) and $OH + Ar \rightarrow O + H + Ar$ (3) rate-constant values came from previous determinations realized with our experimental apparatus [11,18]. The $N_2O + Ar \rightarrow N_2 + O + Ar$ (1) rate-coefficient expression, also used by Natarajan and Roth [1], was chosen in the NIST database [19]. Only one reaction with nitrogen compounds has been considered. In our experimental conditions and with the low N_2O concentration used, N_2 dissociation and reaction with N_2 as a third body could be neglected, and we did not consider reaction with N_2O other than its thermal decomposition. The reverse rate coefficients were obtained from the reaction equilibrium constants, cal-

Table I   Different Test Gas Mixtures Diluted in Argon Used

Mixture	A	B	C
N_2O (ppm)	21	26.3	12
H_2 (ppm)	55.6	67.5	35.1

Table II   Reaction Mechanism and Rate Coefficients Used for the N$_2$O/H$_2$/Ar System

	Reaction	A	n	E/R	Reference
1	N$_2$O + Ar = O + N$_2$ + Ar	9.3×10^{14}	0	29924	[7]
2	O + H$_2$ = OH + H	9.25×10^{14}	0	9740	This work
3	OH + Ar = H + O + Ar	1.20×10^{15}	0	48100	[18]
4	H$_2$ + Ar = 2H + Ar	2.23×10^{14}	0	48350	[15]
5	OH + H$_2$ = H$_2$O + H	1.02×10^8	1.6	1660	[15]
6	H + O$_2$ = OH + O	1.99×10^{14}	0	8460	[4]
7	H$_2$O + Ar = H + OH + Ar	1.26×10^{14}	0	50323	[25]
8	OH + OH = H$_2$O + O	1.50×10^9	1.14	50	[15]
9	O$_2$ + Ar = 2O + Ar	3.40×10^{14}	0	55700	[11]
10	H + HO$_2$ = 2OH	1.69×10^{14}	0	440	[15]
11	H + HO$_2$ = H$_2$ + O$_2$	6.62×10^{13}	0	1070	[16]
12	H + HO$_2$ = H$_2$O + O	1.18×10^{14}	0	1373	[26]
13	2H + H$_2$ = 2H$_2$	9.20×10^{16}	−0.6	0	[27]
14	H$_2$ + O$_2$ = OH + OH	1.70×10^{13}	0	24046	[28]
15	OH + HO$_2$ = H$_2$O + O$_2$	2.89×10^{13}	0	−250	[15]
16	O + HO$_2$ = O$_2$ + OH	1.40×10^{13}	0	540	[27]
17	H + O$_2$ + Ar = HO$_2$ + Ar	6.1×10^{17}	−0.8	0	[15]
18	H$_2$O + H$_2$O = H + OH + H$_2$O	2.27×10^{15}	0	50323	$18 \times k_{Ar}$ [25]
19	H$_2$O$_2$ + H = H$_2$O + OH	2.41×10^{13}	0	2000	[16]
20	H$_2$O$_2$ + H = HO$_2$ + H$_2$	4.80×10^{13}	0	4005	[16]
21	H$_2$O$_2$ + O = HO$_2$ + OH	2.8×10^{13}	0	3220	[29]
22	H$_2$O$_2$ + OH = H$_2$O + HO$_2$	1.00×10^{13}	0	905	[27]
23	H + O$_2$ + H$_2$ = HO$_2$ + H$_2$	2.10×10^{18}	−0.8	0	[15]
24	H + O$_2$ + H$_2$O = HO$_2$ + H$_2$O	1.56×10^{18}	−0.8	0	[4]
25	OH + OH = H$_2$O$_2$	5.80×10^{24}	−3	0	[16]
26	2HO$_2$ = H$_2$O$_2$ + O$_2$	2.00×10^{12}	0	0	[17]

Rate coefficients are expressed in the modified Arrhenius form, $k = AT^n \exp(-E/RT)$. Units are cm^3 mol^{-1} s^{-1} and E/R in K.

culated from the thermochemical database of Burcat and McBride [20].

Sensitivity Analysis

The experimental temperature range was limited at low temperature by the experimental observation time and at high temperature by the possible influence of impurities on the absorption signals. In these limited temperature and pressure ranges, it was necessary to choose optimal initial mixture compositions, respectively, to

  i. obtain O-atom concentrations in the detection limits of the optical arrangement,
 ii. make better use of the ARAS sensitivity,
iii. isolate in these conditions the studied reaction.

Typical O-atom profiles obtained in the N$_2$O/H$_2$/Ar reaction system for a temperature of about 3000 K are shown in Figure 3. First, O atoms were rapidly generated by the fast thermal decomposition of N$_2$O (dur-
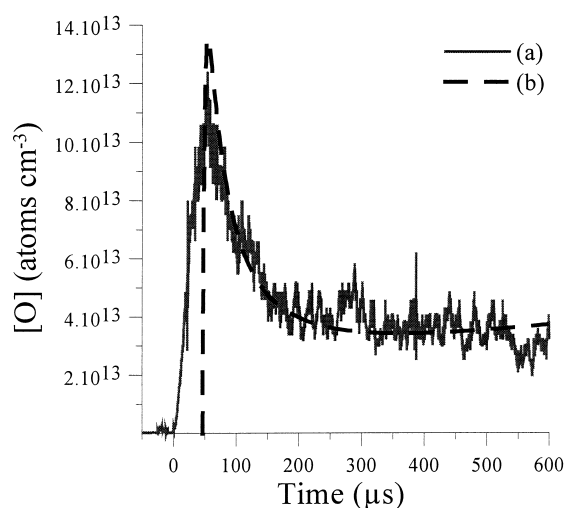
Figure 3   Typical experimental (a) and computed (b) O-atom concentration profiles obtained at 2945 K and 249 kPa with a 26.3 ppm N$_2$O/67.5 ppm H$_2$/Ar mixture.

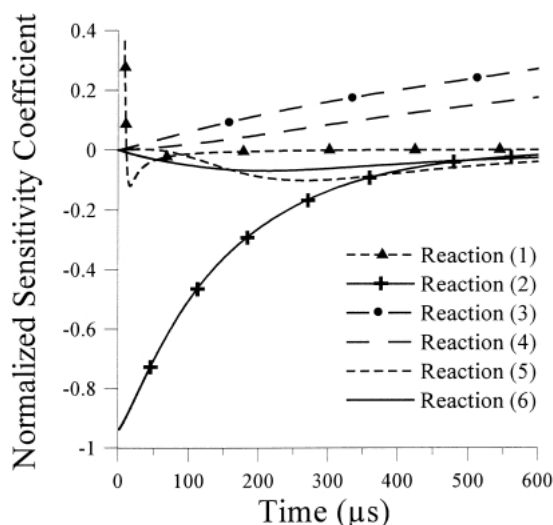**Figure 4** Reaction mechanism sensitivity analysis with respect to the O-atom concentration, obtained at 3000 K and 250 kPa with a 20 ppm N_2O/50 ppm H_2/Ar mixture.

ing the first 50 μs). The grow rate of O atoms and the maximum O concentration obtained depended on both the temperature and the mixture composition. Second, the reaction with H_2 was directly responsible for the decrease of oxygen atoms (until 150 μs). The sensitivity analysis of the reaction mechanism of Table II with respect to the O-atom concentration presented in Figure 4 shows the most important reactions for the oxygen-atom concentration profiles. Only 6 reaction-rate constants of our 26 reaction mechanisms exerted an appreciable influence on the O-atom profiles. Among these reactions, two had the greatest effects on the formation and disappearance of O atoms in the early reaction time: $N_2O + Ar \rightarrow N_2 + O + Ar$ (1) and $O + H_2 \rightarrow OH + H$ (2). From about 250 μs to the end of the observation time, the measured O-atom concentration was primarily sensitive to the OH dissociation rate constant. It justified the use of the k_3 rate constant reevaluated previously [18], which was in agreement with the recommended value of Tsang and Hampson [16]. After 350 μs, the reaction $H_2 + Ar \rightarrow 2H + Ar$ (4) took more part than the studied reaction in the total O-atom concentration, but less than reaction (3). The reactions $H + O_2 = OH + O$ (6) and $OH + H_2 = H_2O + H$ (5) contributed to the O profile between 100 and 350 μs of the reaction time, but less than the studied reaction.

We concluded that the $O + H_2 \rightarrow OH + H$ rate constant could be deduced between the beginning of the O-atom concentration decrease and 150 μs of the observation time. The influence of uncertainties in the

rate coefficient values of the five other reactions on the evaluation of k_2 will be evaluated later on.

Experimental Rate Coefficients and Uncertainties

All experimental data that inferred rate coefficients from O-atom measurements in the N_2O/H_2/Ar reaction system are presented in Table III. The values are plotted in an Arrhenius diagram in Figure 5. Least-squares fitting all points gave with a percentage standard deviation of 8%:

$$k_2(\text{cm}^3 \text{ mol}^{-1} \text{ s}^{-1}) = 9.25 \times 10^{14} \exp(-9740/T(\text{K})).$$

The evaluated preexponential factor ($A = 9.25 \times 10^{14}$ cm^3 mol^{-1} s^{-1}) is very close to the frequency factor calculated at 3000 K, from the gas kinetic theory. By using data of Kee et al. [21], the calculated preexponential factor was found to be approximately equal to 9×10^{14} cm^3 mol^{-1} s^{-1} by assuming a steric factor close to 1.

The evaluated activation temperature ($\theta = 9740$ K) is in very good agreement with those proposed by Shin et al. [3] and Davidson and Hanson [2], respectively, 9382 and 9540 K, in the temperature ranges 1790–2250 and 2120–2750 K. Moreover, considering the three-parameters expression proposed by Natarajan and Roth [1], $k_2(\text{cm}^3 \text{ mol}^{-1} \text{ s}^{-1}) = 3.72 \times 10^6 T^{2.17}(\text{K})$
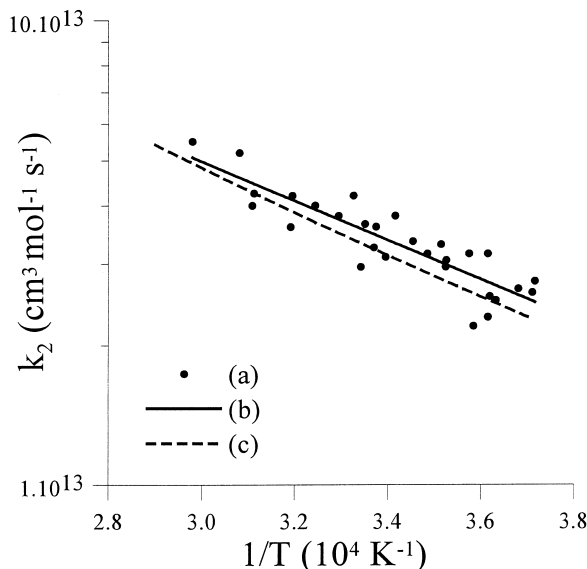

Figure 5 Arrhenius diagram of the experimental data (a) for the reaction $O + H_2 \rightarrow OH + H$. (b) Actual experimental data least-squares fit. (c) Result of Natarajan and Roth [1].

Table III   Experimental Results from O-atom Measurements in the $N_2O/H_2/Ar$ Reaction System

T(K)	P (kPa)	χ_{N_2O} (ppm)/χ_{H_2} (ppm)	k_2(cm^3 mol^{-1} s^{-1})
2691	255	26.3/67.5	2.75×10^{13}
2695	274	21/55.6	2.60×10^{13}
2717	275	21/55.6	2.65×10^{13}
2753	248	26.3/67.5	2.50×10^{13}
2763	273	21/55.6	2.55×10^{13}
2766	257	12/35.1	2.30×10^{13}
2766	271	12/35.1	3.15×10^{13}
2790	249	26.3/67.5	2.20×10^{13}
2797	248	26.3/67.5	3.15×10^{13}
2836	252	12/35.1	3.05×10^{13}
2837	261	12/35.1	2.95×10^{13}
2845	252	21/55.6	3.30×10^{13}
2869	246	26.3/67.5	3.15×10^{13}
2895	261	21/55.6	3.35×10^{13}
2927	269	21/55.6	3.80×10^{13}
2945	249	26.3/67.5	3.10×10^{13}
2963	258	21/55.6	3.60×10^{13}
2967	245	12/35.1	3.25×10^{13}
2984	251	26.3/67.5	3.65×10^{13}
2992	249	21/55.6	2.95×10^{13}
3006	236	26.3/67.5	4.20×10^{13}
3035	268	12/35.1	3.80×10^{13}
3082	258	26.3/67.5	4.00×10^{13}
3129	249	26.3/67.5	4.20×10^{13}
3133	251	26.3/67.5	3.60×10^{13}
3212	262	12/35.1	4.25×10^{13}
3216	252	12/35.1	4.00×10^{13}
3245	248	26.3/67.5	5.20×10^{13}
3356	252	21/55.6	5.50×10^{13}

exp($-4080/T$(K)), within the temperature range 2690–3360 K, the O + $H_2 \rightarrow$ OH + H reaction rate constant can be written k_2(cm^3 mol^{-1} s^{-1}) = 1.14 $\times$ 10^{15} exp($-10565/T$(K)), without significant discrepancy on the k_2 values. With this correlation type, the activation temperature found from the data of Natarajan and Roth [1] is also very close to our experimental value.

Many experimental parameters contributed to uncertainties in the evaluation of the rate constant for reaction (2):

Temperature and Pressure. With our experimental apparatus, we found uncertainty factors of $\pm 0.9\%$ and $\pm 2\%$, respectively, for the calculated temperature and pressure behind the reflected shock waves. In the experimental temperature and pressure ranges used in this study, the variation of the O-atom profiles with temperature and pressure appeared only at the end of

the observation time and was very low compared to the noise signal. Thus we considered the influence of experimental temperature and pressure uncertainties on the evaluation of k_2 negligible.

Mixture Composition. We estimated an error of $\pm 1.3\%$ on the reactive components. It involved a maximum uncertainty of $\pm 5\%$ on the rate-constant evaluation for the studied reaction.

Calibration. An estimated error of $\pm 10\%$ was considered for the calculated O-atom concentrations with the calibration curve. Therefore an uncertainty of about $\pm 15\%$ was found on the determination of k_2.

Reaction Mechanism Rate Coefficients. The rate-coefficient uncertainties concerning the sensitive reactions of the mechanism are given in Table IV and their influence is represented in Figure 6. The variations of

Table IV   Rate Coefficient Uncertainties for the Sensitive Reactions in the $N_2O/H_2/Ar$ System Mechanism

	Reaction	A	n	E/R	Uncertainty (%)	Reference
1	$N_2O + Ar = O + N_2 + Ar$	9.3×10^{14}	0	29924	40	[7]
2	$O + H_2 = OH + H$	9.25×10^{14}	0	9740	33	This work
3	$OH + Ar = O + H + Ar$	1.20×10^{15}	0	48100	50	[18]
4	$H_2 + Ar = 2H + Ar$	2.23×10^{14}	0	48350	30	[15]
5	$OH + H_2 = H_2O + H$	1.02×10^8	1.6	1660	30	[15]
6	$H + O_2 = OH + O$	1.99×10^{14}	0	8460	20	[4]

Rate coefficients are expressed in the modified Arrhenius form, $k = AT^n \exp(-E/RT)$. Units are $cm^3\ mol^{-1}\ s^{-1}$ and E/R in K.

the O-atom profiles enclosed the experimental noise signal and corresponded until 150 μs to a O + H$_2$ → OH + H rate constant correction of about ±8%. We note as Natarajan and Roth [1] that above about 3000 K O-atom concentration profiles go up slowly after 250 μs. From this time, the measured O-atom concentration increase is primarily sensitive to the OH and H$_2$ dissociation reactions (Figs. 4 and 7). The slight discrepancies between experimental and computed profiles obtained in this case are explained by the uncertainties on the reaction rate coefficients.

Initial Reactants, Intermediate Species and Impurities Absorption. Frank and Just [7] and Natarajan and Roth [1] took into consideration the possible absorp-

tion at the O-triplet emission line of species other than O atoms. In this study, the contribution of the intermediate species as well as the reactants to the absorption signal were evaluated by using the absorption cross sections given by Natarajan and Roth [1]. This contribution was calculated to be negligible. The influence of impurities contained in Ar was also estimated. Until 3400 K and during the first 400 μs of the observation time, absorption by impurities was negligible.

The Optical Arrangement. The rapid initial growth of O-atom concentration could not be accurately monitored. We notice also that simulation curves do not
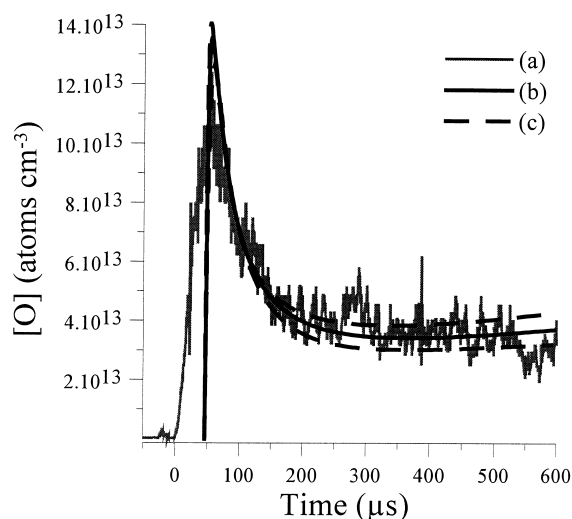

Figure 6   Influence of the reaction rate constant uncertainties for an experiment at 2945 K and 249 kPa, with a 26.3 ppm N$_2$O/67.5 ppm H$_2$/Ar mixture: (a) experimental profile, (b) best computed profile, (c) computed profiles calculated with reaction rate constant uncertainties.
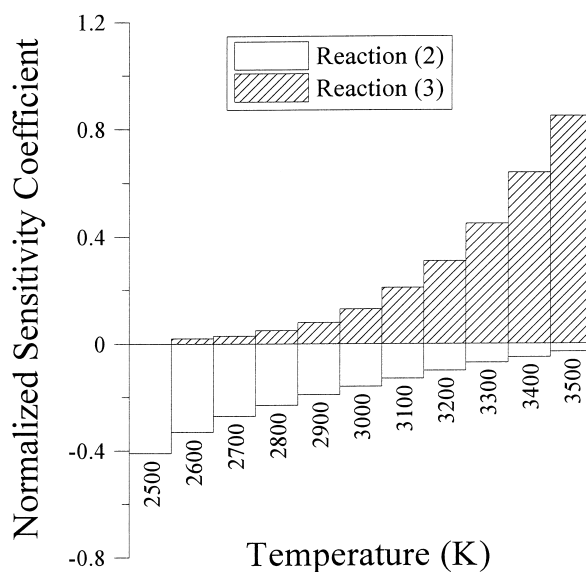

Figure 7   Normalized sensitivity coefficient evolution of the reactions OH + Ar → H + O + Ar (3) and O + H$_2$ → OH + H (2) vs. temperature. Simulation conditions: $t = 250$ μs, 2.5 atm, 20 ppm N$_2$O/50 ppm H$_2$/Ar mixture.

always reproduce properly the experimental maximum O-atom concentrations. Three optical-arrangement parameters are responsible for this deviation:

When the transmitted intensity I approaches zero, the resultant absorbance D comes close to infinity. Hence, the experimental maximum O-atom concentration value is uncertain: $D = \log(I_0/I) = \varepsilon\ell[O]$, where ℓ is the optical path and ε the molar absorption coefficient.

The rise time and the effective light beam width, which depend on the aperture and the slit width of the optical arrangement, also contribute to the discrepancy between experiment and simulation. The faster the initial growth of O-atom concentration is, the higher the gap between experiment and simulation close to the maximum O-atom concentration.

For the rate constant k_2 evaluation, the resultant effect has been taken into account by the adjustment in time between the computed profile and the experimental one. The error has been estimated to be less than ±5%. Note that we chose experimental conditions so that the O-atom decrease rate after the optimal O-atom concentration was slow enough to not introduce significant error on k_2 determination.

In consequence, the overall uncertainty in the rate coefficient expression for the O + H₂ → OH + H reaction was evaluated to be much less than 33%, in the temperature range 2690–3360 K.

DISCUSSION

Figure 8 compares the present rate-constant expression with those reported by earlier investigators at high temperature.

The present result is in good agreement with the three-parameters expression of Natarajan and Roth [1] obtained in the temperature range 1713–3532 K: $k_2(\text{cm}^3 \text{ mol}^{-1} \text{ s}^{-1}) = 3.72 \times 10^6 T^{2.17}(\text{K}) \exp(-4080/T(\text{K}))$. Their experimental results are only 3% lower than ours in the temperature range of 2690 to 3360 K. Their overall uncertainty was estimated to be about ±25%, including only the errors due to the evaluation of experimental temperature and in the optical system calibration procedure. The influence of the reaction-rate coefficient uncertainties was found to be very low.

The reaction mechanism of Natarajan and Roth [1] used for computed simulations was slightly different from ours. In particular, they did not take into account the OH + Ar → O + H + Ar (3) reaction although it exerted an appreciable influence on the O-atom pro-

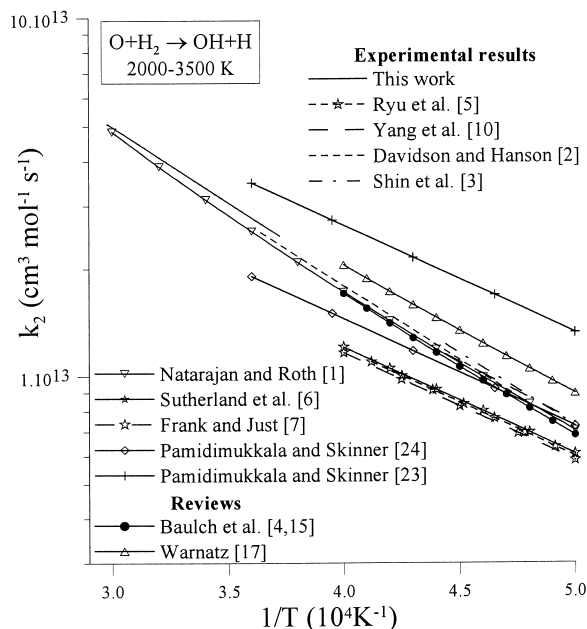**Figure 8** Comparison between the present determination and earlier rate-constant expressions for the reaction O + H₂ → OH + H.

files at temperatures over 2800 K (Fig. 7). Figure 9 compares simulations obtained with the reaction mechanism of Natarajan and Roth [1] and with those of this study. When the OH dissociation reaction is added to their mechanism, the resulting O-atom concentration profile fits very well with ours, which could justify the low deviation found between the present results and theirs.

The experimental conditions used by Frank and Just [7] concerning the O + H₂ → OH + H reaction rate-constant determination have not been given in detail. It is then difficult to discuss their work in comparison to that of Natarajan and Roth [1]. However, the reaction mechanism, the experimental temperature range, and the method used by Natarajan and Roth [1] seemed to be practically identical to those of Frank and Just [7]. The deviation between their results increased from 12% at 1700 K to 34% at 2500 K. So the experimental condition range and the reaction-rate coefficient accuracy did not seem to be the major sources of uncertainty. The discrepancy was probably inherent to the absorption technique.

In the studied temperature range, the rate constant for reaction (2) presented an Arrhenius behavior versus temperature. So, between 2690 and 3360 K, the temperature dependence of the activation energy seemed to be negligible, as pointed out by Gardiner et al. [22]. Thus, contrary to Natarajan and Roth [1], who
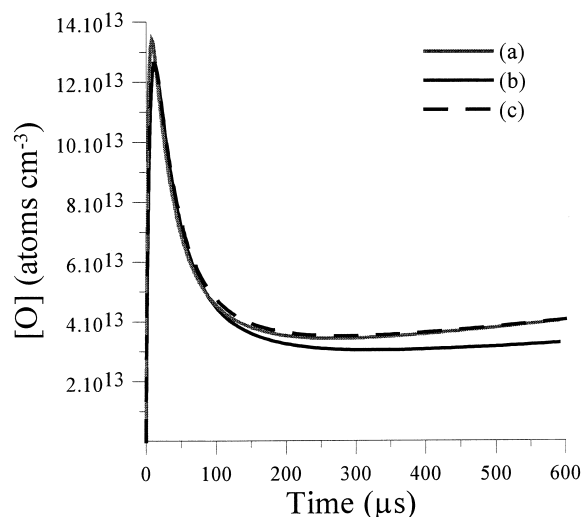
Figure 9 Comparison between (a) the mechanism used in this study, (b) the mechanism of Natarajan and Roth, and (c) the mechanism of Natarajan and Roth with reaction (3) added. Computed simulations at 2945 K and 249 kPa, with a 26.3 ppm N_2O/67.5 ppm H_2/Ar mixture.

had worked in a larger temperature range, we do not propose a three-parameter expression for k_2.

The present study is in continuity with the previous photolysis and pyrolysis shock tube investigation of Davidson and Hanson [2]. The differences between the results reported in this study and the extrapolation at higher temperatures given by Shin et al. [3] or recommended by Baulch et al. [4,15] and Warnatz [17] also do not exceed 3%.

On the other hand, by comparison with the extension at higher temperature of the recent study of Ryu et al. [5] and the earlier determinations of Sutherland et al. [6] and Frank and Just [7], we find a percentage deviation of about -30%, which corresponds to our overall uncertainty. The results of Ryu et al. [5] confirmed the theoretical calculations of Bowman et al. [8] and Garrett and Truhlar [9]. All of these studies were performed at lower temperatures (200–2500 K) than ours (2690–3360 K) and the non-Arrhenius behavior of the rate constant k_2 versus temperature has notably been pointed out by several investigators. It can be an explanation for the discrepancy between the results.

Pamidimukkala and Skinner [23,24] proposed the same activation temperature as Sutherland et al. [6], Frank and Just [7], and Ryu et al. [5], but a higher exponential factor. The deviation between the present result and those of Pamidimukkala and Skinner [23,24] is about $+22$ and -8%, respectively. Yang et al. [10] proposed intermediate rate coefficients: k_2(cm^3

mol^{-1} s^{-1}) $= 3.7 \times 10^{14} \exp(-7818/T(K))$, with an estimated error of $\pm15\%$, including the dependence on the rate coefficients assigned to the other reactions in the mechanism. These results are only 13% lower than ours.

CONCLUSION

Resonance Absorption measurements of O atoms have been used to obtain new experimental results for the reaction $O + H_2 \rightarrow OH + H$ in the temperature range of 2690 to 3360 K, using N_2O/H_2/Ar mixtures. The rate constant for this reaction reported in the present study is in good agreement with the recommended value of Baulch et al. [4]. We confirmed at temperatures over 2700 K the result previously reported by Natarajan and Roth [1], also obtained by O-ARAS measurements. The dependence of the activation energy with temperature has not been observed between 2690 and 3360 K.

BIBLIOGRAPHY

1. Natarajan, K.; Roth, P. Combust Flame 1987, 70, 267–279.
2. Davidson, D. F.; Hanson, R. K. Combust Flame 1990, 82, 445–447.
3. Shin, K. S.; Fujii, N.; Gardiner, W. C., Jr. Chem Phys Lett 1989, 161, 219–222.
4. Baulch, D. L.; Cobos, C. J.; Cox, R. A.; Esser, C.; Frank, P.; Just, Th.; Kerr, J. A.; Pilling, M. J.; Troe, J.; Walker, R. W.; Warnatz, J. J Phys Chem Ref Data 1992, 21, 411–429.
5. Ryu, S. O.; Hwang, S. M.; Rabinowitz, M. J. Chem Phys Lett 1995, 242, 279–284.
6. Sutherland, J. W.; Michael, J. V.; Pirraglia, A. N.; Nesbitt, F. L.; Klemm, R. B. Twenty-First Symposium (International) on Combustion; The Combustion Institute: Pittsburgh, PA, 1986, pp 929–941.
7. Frank, P.; Just, Th. Ber Bunsenges Physik Chem 1985, 89, 181–187.
8. Bowman, J. M.; Wagner, A. F.; Walch, S. P.; Dunning, T. H., Jr. J Chem Phys 1984, 81, 1739–1752.
9. Garrett, B. C.; Truhlar, D. G. Int J Quant Chem 1986, 29, 1463–1482.
10. Yang, H. X.; Shin, K. S.; Gardiner, W. Chem Phys Lett 1993, 207, 69–74.
11. Naudet, V.; Abid, S.; Paillard, C. E. J Chim Phys 1999, 96, 1123–1145.
12. Just, T. In Shock Waves in Chemistry; Lifshitz, A., Ed.; Dekker: New York and Basel, 1981; Chapter 6.
13. Lutz, A. E.; Kee, R. J.; Miller, J. A. SENKIN II, Version 2.3, Sandia International Laboratories Report No. SAND87-8248, 1991.
14. Catoire, L.; Bassin, X.; Ingignoli, W.; Dupré, G.; Paillard, C. E. Combust Flame 1997, 109, 37–42.

15. Baulch, D. L.; Cobos, C. J.; Cox, R. A.; Frank, P.; Hayman, G.; Just, Th.; Kerr, J. A.; Murrels, T.; Pilling, M. J.; Troe, J.; Walker, R. W.; Warnatz, J. Combust Flame 1994, 98, 59–79.

16. Tsang, W.; Hampson, R. F. J Phys Chem Ref Data 1986, 15, 1087–1279.

17. Warnatz, J. In Combustion Chemistry; Gardiner, W. C., Jr. , Ed.; Springer-Verlag: New York, 1984; Chapter 5.

18. Naudet, V.; Javoy, S.; Paillard, C. E. Submitted.

19. Mallard, W. G.; Westley, F.; Herron, J. T.; Hampson, R. F. NIST Standard Reference Database 17, Chemical Kinetics Database-Version 6.01; Gaitherburg, MD, 1994.

20. Burcat, A.; McBride, B. 1995 Ideal Gas Thermodynamic Data for Combustion and Air-Pollution Use, Technion-Israel Institute of Technology, TAE 732, 1995.

21. Kee, R. J.; Dixon-Lewis, G.; Warnatz, J.; Coltrin, M. E.; Miller, J. A. A Fortran Computer Code Package for the Evaluation of Gas-Phase, Multicomponent Transport Properties, 1986.

22. Gardiner, W. C., Jr.; Mallard, W. G.; McFarland, M.; Morinaga, K.; Owen, J. H.; Rawlins, W. T.; Takeyama, T.; Walker, B. F. Fourteenth Symposium (International) on Combustion; The Combustion Institute: Pittsburgh, PA, 1973; pp 61–75.

23. Pamidimukkala, K. M.; Skinner, G. B. J Chem Phys 1982, 76, 311–315.

24. Pamidimukkala, K. M.; Skinner, G. B. Thirteenth Proc Int Symp Shock Tubes Waves 1985, 585–592.

25. Bopp, J. M.; Kern, R. D.; Niki, T. J Phys Chem 1978, 82, 1343–1346.

26. Dagaut, P.; Cathonnet, M.; Boettner, J.-C. Int J Chem Kinet 1991, 23, 437–455.

27. Miller, J. A.; Bowman, C. T. Prog Energy Combust Sci Technol 1989, 15, 287–338.

28. Dagaut, P.; Boettner, J.-C.; Cathonnet, M. Combust Sci Technol 1991, 77, 127–148.

29. Albers, E. A.; Hoyermann, K.; Wagner, H. G.; Wolfrum, J. Thirteenth Symposium (International) on Combustion; The Combustion Institute: Pittsburgh, PA, 1971; pp 81–88.